of the effect, but for the above case, ~2 cm of lead will stop sky shine and other scattered radiation.

In addition to the primary radiation hazards of microwaves and x-rays, most HPM research facilities have other safety issues that must be addressed: (1) high voltage in the pulsed power system; (2) use of insulating sulfur hexafluoride (SF_6) gas, to be used and vented in a controlled manner; and (3) hazardous materials, most especially oil for insulation, which raises the issue of oil fires and oil containment in berms.

Problems

1. The highest energy or power transfer efficiency between pulsed power elements such as pulse lines occurs when the lines are matched in impedance. Mismatching upward, to higher impedance, gives higher voltage but lower current. If that line in turn drives a beam-generating Child–Langmuir diode ($I \sim V^{3/2}$, $Z \sim V^{-1/2}$), will the microwave power be greater than in the matched case?
2. Some types of vircators begin radiating microwaves when the electron beam starts to pinch in the diode, launching electrons on converging trajectories beyond the anode. This increases the density and forms the virtual cathode. This is when the Child–Langmuir current equals the pinch current. For operation at 0.5 MeV, what diode aspect ratio r_c/d is required for starting microwaves? What is the diode impedance?
3. An X-band antenna has a beam width of 18°. If its efficiency is 50%, what is its gain?
4. To produce 1 kW/cm^2 at a range of 1 km, what effective radiated power (ERP) is required? If the source has 10 GW of peak power, what gain antenna is needed? If the antenna efficiency is 80% and the diameter is 10 m, what is the highest power you can radiate without air breakdown? If it is raining heavily at 16 mm/h, what attenuation will the beam experience if the frequency is 10 GHz?
5. What power density can be produced at a 100-m range from a conical horn operating at 1 GHz? Estimate what power can be radiated at sea level if the only limit is atmospheric breakdown.
6. If you have a source that chirps upward in frequency, increasing 20% during the pulse, which of the frequency diagnostic methods discussed here (bandpass filters, dispersive line, hetrodyne, time–frequency analysis) would you use?
7. The Orion test facility has an effective antenna diameter of 2.5 m. If the target is 100 m away and is 10 m wide, and you are using a 1-GHz beam with 500 MW of power, is the target in the far field of the antenna? What is the power density on the target? If you need to place 90% of the power on target, what could you do? Discuss the practicality of your approach.

Further Reading

Pulsed power topics are described best in the biannual proceedings of the IEEE Pulsed Power Conference. There is also a series of books on special topics edited by Mesyats, Pai, Vitkovitsky, DiCapua, Guenther, and Altgilbers.[1–3,5,6] A comprehensive tome on beams is Humphries,[16] and the best on antennas is Balanis.[27] The best survey of plasma diagnostics is by Hutchinson.[42]

References

1. Mesyats, G.A., *Pulsed Power*, Kluwer Academic/Plenum Publishers, New York, 2005.
2. Pai, S.T. and Zhang, Q., *Introduction to Pulsed Power*, World Scientific, Singapore, 1995.
3. Vitkovitsky, I., *High Power Switching*, Van Nostrand Reinhold Co., New York, 1987.
4. DiCapua, M.S., Magnetically insulated transmission lines, *IEEE Trans. Plasma Sci.*, PS-11, 205, 1983.
5. Guenther, A., Kristiansen, M., and Martin, T., *Opening Switches*, Plenum Press, New York, 1987.
6. Altgilbers, L.L. et al., *Magnetocumulative Generators*, Springer-Verlag, New York, 2000.
7. Neuber, A.A. and Dickens, J.C., Magnetic flux compression generators, *Proc. IEEE*, 92, 1205, 2004.
8. Maenchen, J. et al., Advances in pulsed power-driven radiography systems, *Proc. IEEE*, 92, 1021, 2004.
9. Bugaev, P.S. et al., Explosive electron emission, *Sov. Phys. Usp.*, 18, 51, 1975.
10. Barker, R.J. and Schamiloglu, E., Eds., *High Power Microwave Sources and Technologies*, IEEE/Wiley Press, New York, 2001, chap. 9.
11. Barker, R.J. et al., *Modern Microwave and Millimeter-Wave Power Electronics*, IEEE Press, New York, 2005, chap. 13.
12. Barletta, W.A. et al., Enhancing the brightness of high current electron guns, *Nucl. Instrum. Meth.*, A250, 80, 1986.
13. Barker, R.J. et al., *Modern Microwave and Millimeter-Wave Power Electronics*, IEEE Press, New York, 2005, chap. 8.
14. Thomas, R.E., Thermionic sources for hi-brightness electron guns, in *AIP Conference Proceedings 188*, 1989, p. 191.
15. Oettinger, P.E. et al., Photoelectron sources: selection and analysis, *Nucl. Instrum. Meth.*, A272, 264, 1988.

16. Humphries, S., *Principles of Charged Particle Acceleration*, John Wiley & Sons, New York, 1986.
17. Alvarez, R. et al., Application of microwave energy compression to particle accelerators, *Particle Accelerators*, 11, 125, 1981.
18. Birx, D. et al., Microwave power gain utilizing superconducting resonant energy storage, *Appl. Phys. Lett.*, 32, 68, 1978.
19. Devyatkov, N. et al., Formation of powerful pulses with accumulation of uhf energy in a resonator, *Radiotechnika Elektronika*, 25, 1227, 1980.
20. Alvarez, R.R., Byrne, D., and Johnson, R., Prepulse suppression in microwave pulse-compression cavities, *Rev. Sci. Instrum.*, 57, 2475, 1986.
21. Grigoryev, V., Experimental and theoretical investigations of generation of electromagnetic emission in the vircators, in *BEAMS'90*, Novosibirsk, Russia, 1991, p. 1211.
22. Farkas, Z. et al., Radio frequency pulse compression experiments at SLAC, *SPIE*, 1407, 502, 1991.
23. Montgomery, C.G., Dicke, R.H., and Purcell, E.M., *Principles of Microwave Circuits*, Peter Peregrinus Ltd., London, 1987, chap. 10.
24. Thumm, M.K. and Kasparek, W., Passive high-power microwave components, *IEEE Trans. Plasma Sci.*, 30, 755, 2002.
25. Vlasov, S.N., Zagryadskaya, L.I., and Petelin, M.I., Transformation of a whispering gallery mode, propagating in a circular waveguide, into a beam of waves, *Radio Eng. Elec. Phys.*, 20, 14, 1975.
26. Fenstermacher, D.L. and von Hippel, F., Atmospheric limit on nuclear-powered microwave weapons, *Sci. Global Security*, 2, 301, 1991.
27. Balanis, C.A., *Antenna Theory*, 2nd ed., John Wiley & Sons, New York, 1997.
28. Sze, H. et al., Operating characteristics of a relativistic magnetron with a washer cathode, *IEEE Trans. Plasma Sci.*, PS-15, 327, 1987.
29. Vlasov, S.N. et al., Transformation of an axisymmetric waveguide mode into a linearly polarized Gaussian beam by a smoothly bent elliptic waveguide, *Sov. Tech. Phys. Lett.*, 18, 430, 1992.
30. Sze, H. et al., A radially and axially extracted virtual-cathode oscillator, *IEEE Trans. Plasma Sci.*, PS-13, 492, 1985.
31. Palevsky, A. and Bekefi, G., Microwave emission from pulsed relativistic e-beam diodes. II. The relativistic magnetron, *Phys. Fluids*, 22, 985, 1979.
32. Price, D. et al., Operational features and microwave characteristics of the vircator II experiment, *IEEE Trans. Plasma Sci.*, 16, 177, 1988.
33. Barker, R.J. and Schamiloglu, E., Eds., *High-Power Microwave Sources and Technologies*, IEEE Press, New York, 2001, chap. 5.
34. Smith, R.R. et al., Direct experimental observation of π-mode oscillation in a relativistic magnetron, *IEEE Trans. Plasma Sci.*, 16, 234, 1988.
35. Friedman, M. et al., Externally modulated intense relativistic electron beams, *J. Appl. Phys.*, 64, 3353, 1988.
36. Early, L.M., Ballard, W.P., and Wharton, C.B., Comprehensive approach for diagnosing intense single-pulse microwave pulses, *Rev. Sci. Instrum.*, 57, 2293, 1986.
37. Sabath, F. et al., Overview of four European high-power narrow-band test facilities, *IEEE Trans. Electromag. Compat.*, 46, 329, 2004.
38. Price, D., Levine, J.S., and Benford, J., ORION: A Frequency-Agile HPM Field Test System, paper presented at the 7th National Conference on High Power Microwave Technology, Laurel, MD, 1997.
39. Hammon, J., Lam, S.K., and Pomeroy, S., Transportable 500 kV, High Average Power Modulator with Pulse Length Adjustable from 100 ns to 500 ns, Proceedings of the 22nd IEEE Power Modulator Symp., Boca Raton, FL, 1996.
40. Lerner, E.J., RF radiation: biological effects, *IEEE Spectrum*, 68, 141, 1980.
41. Recommendations of the National Council on Radiation Protection and Measurements, Radiation Protection Design Guidelines for 0.1–100 MeV Particle Accelerator Facilities, NCR Report 51, 1979.
42. Hutchinson, I., *Principles of Plasma Diagnostics*, 2nd ed., Cambridge Univeristy Press, Cambridge, U.K., 2002.

6

Ultrawideband Systems

6.1 Ultrawideband Defined

Ultrawideband (UWB) high power microwave (HPM) sources are quite different from the narrowband sources described in Chapters 7 to 10. The technology grew out of studies of the electromagnetic pulse (EMP) generated by high-altitude nuclear explosions in the 1960s. Technology developments of the last two decades led to the first UWB pulsers capable of transmitting high-peak field signals through a variety of efficient antennas. This chapter briefly reviews the field. Good references are the book by Giri[1] and review articles by Agee et al.[2] and Prather.[3]

What distinguishes UWB? Its spectral density, the power emitted into any narrow-frequency interval, is very low. Figure 6.1 shows typical spectral magnitudes of electric fields, or E-fields, over a wide range of frequency. (This is a *frequency-domain* plot, as distinct from the better-known *time-domain* plot, which shows amplitude vs. time.) It gives perspective on the relation between the regions of HPM: the lower-frequency continuous spectra from natural lightning and high-altitude electromagnetic pulse (HEMP) together with higher-frequency narrowband HPM, including wideband spectra, the so-called ultrawideband.

UWB sources and antennas are of interest for a variety of potential applications that range from jammers to detection of buried objects and space objects, ultrashort radar systems to industrial and law enforcement applications. As a directed energy weapon, UWB offers the prospect of making high electric fields available across a wide range of frequencies to take advantage of coupling mechanisms and internal electronic vulnerabilities at frequencies that are not known *a priori*. The disadvantage of this approach is that in spreading the energy over a wide band of frequencies, the amount of energy actually coupled into a system is reduced by the ratio of the coupling bandwidth divided by the UWB system bandwidth, or a sum of such ratios if multiple coupling bands are available over the full UWB system bandwidth. Many military assets and civilian systems (e.g., nuclear power plants, communications facilities) are suspected of being vulnerable to the effects of

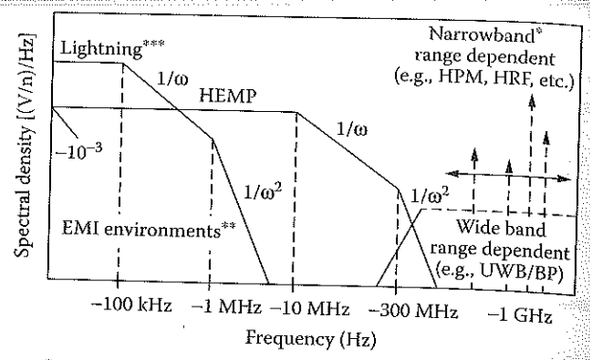

*narrowband extenting from 1.5 to 3 GHz
**not necessary HPEM
***significant spectral components up to 20 MHz depending on range

FIGURE 6.1
Spectral domains of electromagnetic pulse types. (Reprinted from Giri, D.V. and Tesche, F.M., *IEEE Trans. Electromag. Compat.*, 46, 2, 2004, Figure 1. By permission of IEEE.)

UWB, which would most likely mean interruption and jamming rather than destruction, because the total system energy is spread over such a broad frequency range, while the coupling and vulnerability bandwidths are typically quite narrow.

The types of microwave pulses termed UWB are very different from narrowband microwaves in both the frequency spectrum and the technologies used to generate them. In fact, the UWB terminology has become dated and is being superceded by the more specific terms in Table 6.1, which shows the classification of pulses based on bandwidth.[4] Why are the distinctions between the subbands of UWB important? Because they differ quite a lot in their coupling into electronics, their effects on electronics, and use rather different technologies.

Bandwidth by definition is the half width of power in frequency space; the low- and high-frequency limits are half-power points (3 dB down) from

TABLE 6.1

HPM Band Regions

Bands		Percent Bandwidth, 100 Δf/f	Bandwidth Ratio, 1 + Δf/f	Example
Narrowband		<1%	1.01	Orion (Figures 5.31 and 7.24)
Ultrawideband	Moderate band (mesoband)	1–100%	1.01–3	MATRIX (Figure 6.11)
	Ultramoderate band (subhyperband)	100–163%	3–10	H-Series (Figure 6.16)
	Hyperband	163–200%	>10	Jolt (Figure 6.17)

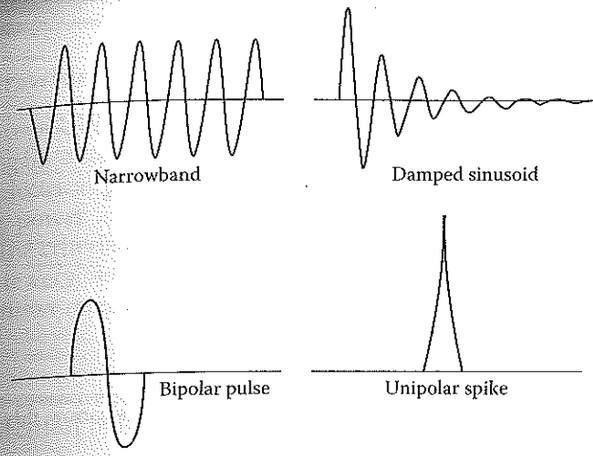

FIGURE 6.2
Electric fields of classes of pulses. As the number of cycles increases, the bandwidth decreases. (a) Narrowband; (b) damped sinusoid; (c) bipolar pulse; (d) unipolar spike (which does not radiate as a spike, but as a cycle).

the power peak. (A more general definition is the frequency range that contains a large fraction of the pulse energy, for example, 90%.) If the frequencies are separated by f, the widely used definitions for bandwidth are fractional bandwidth Δf/f, sometimes expressed as percentage bandwidth, 100 Δf/f, and bandwidth ratio, 1 + Δf/f (see Problem 1).

Figure 6.2 shows several types of pulses from narrowband to a simple voltage spike. The narrow band is a long series of cycles, giving a relatively narrow bandwidth, usually defined as Δf/f~1%. The next most similar waveform is the damped sinusoid, a finite number of cycles. The most common UWB pulse is bipolar, and the ultimate is a single unipolar spike. The frequency spectrum changes accordingly (Figure 6.3). As the number of cycles decreases, the bandwidth increases. The spectrum changes from narrow, when there are many cycles available to determine the frequency, to broad for shorter pulses. (Mathematically, time and frequency are conjugate variables; the narrower in either time or frequency, the broader you are in the conjugate variable.) The number of cycles, the bandwidth, BW, and the Q of the resonant system that produces the pulse (see Chapter 4) are related by

$$N = 1/\text{percentage BW} = Q \qquad (6.1)$$

However, for single cycle pulses, these quantities are not useful (see Problem 2).

Technologywise, going from narrowband to UWB means a transition from electron beam devices to devices in which fast switches direct the pulsed power output directly to an antenna. The wideband spectrum requires a constant, or nearly constant, gain antenna over a broad frequency range.

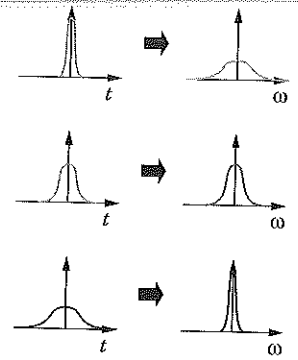

FIGURE 6.3
Time and frequency descriptions of short unipolar pulses. As pulses narrow, they have wider bandwidth.

This is quite difficult to do because antenna gain normally depends strongly upon frequency. The approach now used is to have pulsed power generate a fast rising step in voltage. This is connected to a differentiating antenna (one that produces the time derivative of the incoming pulse), which converts the voltage step into an electric field spike in the radiation field. The antenna of choice in the UWB community is the Impulse Radiating Antenna (IRA).

For narrowband microwave sources, the requirement for a resonance involving a beam of monoenergetic electrons is that the pulsed power must generate a relatively long flat-top voltage pulse. Since the source is narrowband, the antenna can be optimized for the operating frequency.

But for UWB, pulsed power must generate a short voltage spike. The antenna aperture area is typically limited to the area $A < 10\ m^2$, for example, by the requirement that it can be truck mounted. For such an antenna radiating a peak power P, the average E-field in the aperture of the antenna is

$$E_0 = \sqrt{\frac{PZ_o}{A}} \tag{6.2}$$

where Z_0 is the impedance of free space, 377Ω. But as we shall see, *for UWB the peak-radiated E-field at a distance R depends on the rate of rise of voltage.* The widely used *figure of merit for UWB is the far voltage* (sometimes called *far-field voltage*), the range-normalized peak-radiated E-field (somewhat like the effective radiated power [ERP; see Chapter 5] for narrowband) is

$$V_f = RE_p \tag{6.3}$$

Values are typically of the order 100 kV, but 5 MV has been achieved (see Section 6.4.3).

6.2 Ultrawideband Switching Technologies

The essence of UWB technology is extremely fast switching and nondispersive high-gain antennas. The pulsed power section of a UWB device is a series of electrical pulse compression stages, generating shorter pulses at increasing power as the signal proceeds through the system toward the antenna. The criteria for the switching element are ultrafast closing capability to create very fast rising waveforms, and rapid voltage recovery, so that high repetition rates are achievable.[2] The principal switching technologies used are:

- High-pressure gas or liquid spark gap switches, typically triggered by electrical pulses
- Photoconductive semiconductor switches, which are triggered by lasers

6.2.1 Spark Gap Switches

A fast rising pulse is critical because the rise time determines the high-frequency components of the transmitted spectrum in an antenna such as the IRA, which responds to the derivative of the signal applied to it. To sharpen the rise time on a pulse, a peaking switch may be used. Such switches have been developed since the early 1970s in electromagnetic pulse (EMP) simulators. The essence of the peaking gap is establishment of very high electric fields between very closely spaced electrodes. Contemporary spark channels have gap lengths of 1 mm. Because of the short gap lengths, charge voltages of less than 100 kV can produce spark gap electric fields in excess of MV/cm, resulting in very fast breakdown of the gap.

Spark gaps proceed through several brief intervals: capacitive phase before breakdown and arc formation, resistive phase as the gas channel heats, and an arc phase when the switch is fully closed. The latter is inductive, and very low inductance is essential, less than 1 nH. The rise time is governed by both resistive and inductive times:

$$\tau = \sqrt{\tau_r^2 + \tau_L^2} \tag{6.4}$$

$$\tau_r = \frac{88ns}{Z^{1/3}E^{4/3}}\rho^{1/2} \tag{6.5}$$

$$\tau_L = \frac{L_c + L_h}{Z} \tag{6.6}$$

TABLE 6.2

H-Series of Mesoband Generators

Generator	Operating Voltage, V_0 (kV)	10–90 Rise Time (psec)	dV/dt (kV/sec)	Far Voltage, RE_p (kV), Equation 6.3	Far Voltage/ Source Voltage, RE_p/V_0
H-2	300	250	1.2×10^{15}	350	1.16
H-3	1000	120	8.3×10^{15}	360	0.36
H-5	250	235	1.1×10^{15}	430	1.72

Here Z is the circuit impedance, E the field in the switch, and ρ the gas density in units of atmospheres, and the inductances are those of the arc channel and the housing of the switch. Short gaps mean high electric fields to minimize the resistive phase and, since inductance is proportional to length, the inductive phase as well. The extremely small interelectrode distances do yield high capacitance, even though electrodes are small in area. High-spark-gap capacitance and fast charging times lead to a strong displacement current that produces an undesirable prepulse on the downstream electrode. If not suppressed, it can cause unwanted, lower-frequency components to be radiated before the main pulse.

Both oil and gas are used as insulating media for fast switches. To produce ultrafast switching, the spark gap is dramatically overvolted; that is, the spark gap is charged far in excess of its self-breakdown voltage, which is determined by the gap geometry and pressure. To hold off breakdown, gas UWB gaps operate at pressures in the range of 100 atm. Overvoltages of more than 300% of the self-breakdown voltage are achievable.

High-pressure hydrogen is the gas of choice for high-repetition-rate, peaking UWB switches. Hydrogen has the advantages of supporting higher electric fields and faster recovery time over other atomic gases, in part because it has high ionization energy.

In the 1990s, the H-Series devices developed high-pressure hydrogen switches to produce powerful and very compact mesoband sources. The performance of several H devices, by Air Force Research Laboratory (AFRL) of Albuquerque, can be seen in Table 6.2. Figure 6.4 shows the pulsed power configuration and hydrogen switch in the H-2 system. Pulse compression and voltage multiplication from the initial capacitive store (not shown) occur via the capacitive store/transformer, and the hydrogen switch sends the short pulse onto the antenna. The H-2 generated a 300-kV pulse in a 10-cm-diameter, 40-Ω line with a rise time of about 250 psec and a total pulse length of 1.5 to 2 nsec. This provided an ultrawide spectrum with its center frequency around 150 MHz from a large TEM horn. The H-3 device generated nearly 1 MV into a 40-Ω coaxial line. To achieve the very fast rise time, the H-3 uses a multichannel output switch (Figure 6.5). (Multiple channels lower the switch inductance.) The unique transmission line-to-transmission line-charging technique compresses the pulse and increases the voltage. The first transmission line is charged relatively slowly, then is switched into the

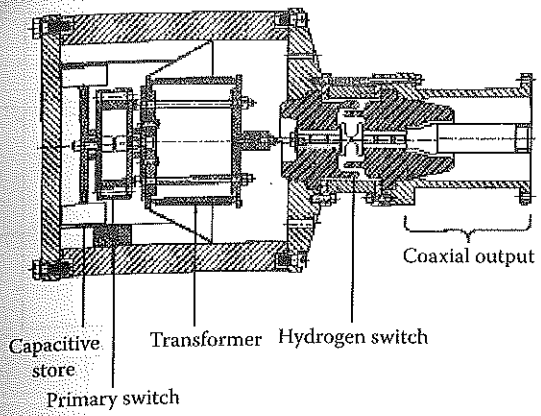

FIGURE 6.4
H-2 hydrogen switch, about 0.5 m long, 0.3 m in diameter. (Reprinted from Agee, F.J. et al., *IEEE Trans. Plasma Sci.*, 26, 863, 1998, Figure 1. By permission of IEEE.)

second line using a high-pressure hydrogen spark gap. The fast charging of the second transmission line creates a large overvoltage on the high-pressure hydrogen, multichannel, ring-gap switch. The radiated field from H-3 has a rise time of 130 psec and pulse duration of 300 psec, as shown in Figure 6.6. The radiated field was generated using a 0.4-m TEM horn with a peak voltage of 130 kV. The field at 6 m was 60 kV/m. The H-5 is a higher-power version of H-2. Figure 6.7 gives the pulse shape and spectrum. Note the broadband spectrum with substantial variations. The bandwidths of such spectra are difficult to clearly define (see Giri[1] and Section 6.1).

Liquid switches have their own issues. When various types of hydrocarbon oil break down, the streamer in the oil leaves a long-lived, electrically

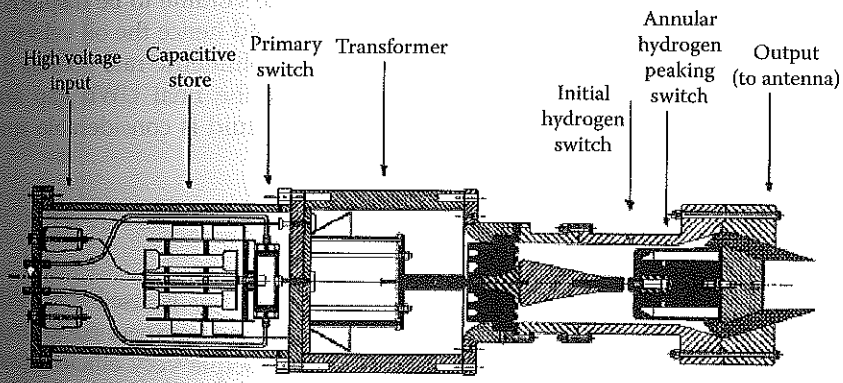

FIGURE 6.5
Schematic of the H-3 source. Note stages of pulse compression using a sequence of switches to produce faster pulses. (Reprinted from Agee, F.J. et al., *IEEE Trans. Plasma Sci.*, 26, 864, 1998, Figure 3. By permission of IEEE.)

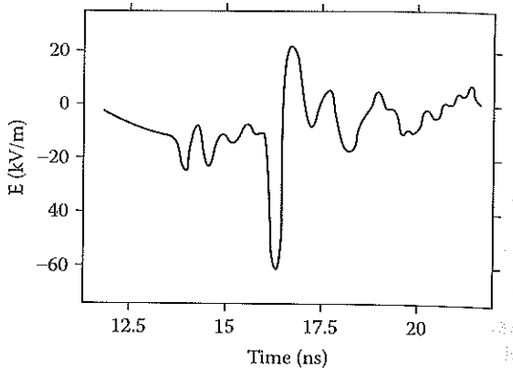

FIGURE 6.6
Field radiated from the H-3 source. (Reprinted from Agee, F.J. et al., *IEEE Trans. Plasma Sci.*, 26, 864, 1998, Figure 4. By permission of IEEE.)

charged streamer containing breakdown by-products that then leave the oil with decreased breakdown strength. The oil recovers more slowly, which limits the possible repetition rate. Titan Pulse Sciences led development of high-repetition-rate oil switches, producing a modulator that contained three oil switches: a transfer switch, a sharpening switch, and a peaking/sharpening switch.[5] The modulator produced pulses with a 10 to 90% rise time of 100 psec, 200-kV pulses at 1500 Hz, as well as 450-kV pulses at 500 Hz.

The Titan Pulse Sciences work investigated the recovery of switches with the direction and rate of oil flow as parameters. If the flow is fast enough to displace a sufficient amount of oil in the gap region, the switch breakdown strength is that of a single pulse, even in repetitive operation. The oil flow rate is a strong function of the switch gap d. The region in the gap of highly stressed oil must be displaced between pulses; the volume to be displaced is proportional to d^3. The displacement distance, and hence the oil velocity, is proportional to d. Therefore, the replacement volumetric rate goes as d^4 (see Problem 3). The flow-rate requirements for the final UWB gap are practically realizable, and the power to drive the fluid is considerable and so may limit the repetition rate.

6.2.2 Solid-State Switches

Photoconductive solid-state (PCSS) switching technology is used for UWB because of very low turn-on jitter, fast rise times, and compact packaging. Such switching has advantages in that it is in principle very efficient (but not in practice), has fewer conversion steps, may allow a degree of agility in frequency and pulse width, and can be used in arrays by phasing of many modules of lower-power units. The principal limitation is power-handling capability. The most likely application is impulse radar because of the low

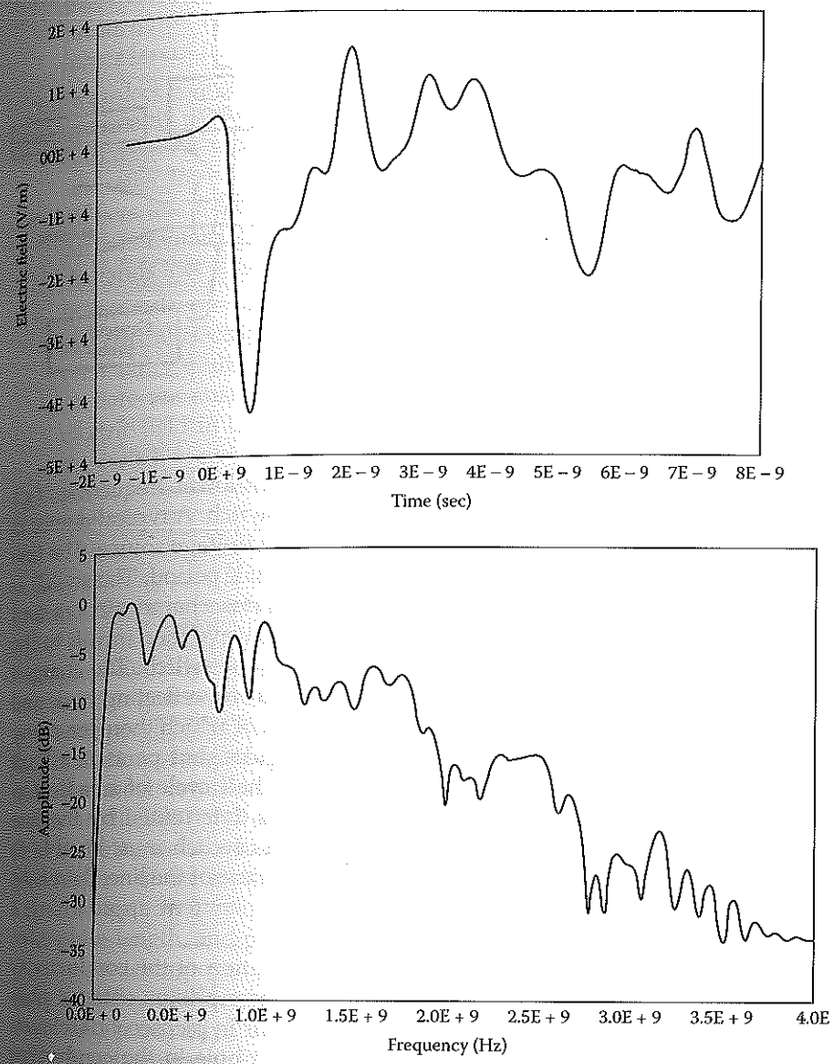

FIGURE 6.7
Radiated field of H-5 at 10 m using a large TEM horn. (Reprinted from Agee, F.J. et al., *IEEE Trans. Plasma Sci.*, 26, 865, 1998, Figure 5. By permission of IEEE.)

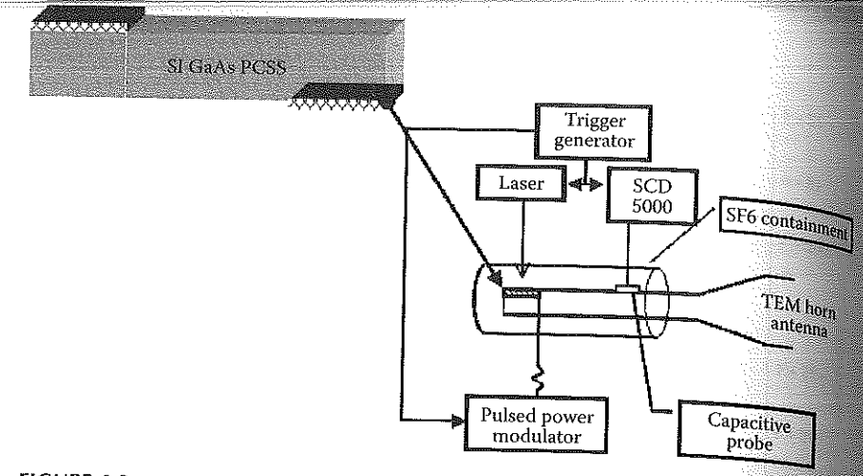

FIGURE 6.8
Schematic of a UWB device driven by a solid-state switch.

energy needed per pulse. The technique is used for lower frequencies (≤1 GHz) to ease laser rise time requirements on the switch. A typical device is shown in Figure 6.8. A pulse line is charged from a voltage source. The line has a transit time equal to the desired microwave half period. The switch is triggered by the laser, which photonically generates charge carriers and connects the center conductor to ground. A voltage wave then travels to the open end of the line, doubles, and reflects back to the switch. The charged line is connected to an antenna and a series of pulses, reflecting back and forth, give a few cycles. This is a mesoband source, of which there are many examples.[6–8] Ideally, the pulses would be rectangular, but parasitic circuit elements produce a rounded profile much like a half cycle of a radio frequency (RF) wave. The amplitude of the wave is determined by the line voltage, and the frequency by the line length. The switch must be able to close in a time that is short compared to the transit time of the line; therefore, subnanosecond switching is essential if frequency content approaching a gigahertz or more is desired.

The photoconductive switch operates by modulation of the conductivity of a semiconductor by photoionization. When a laser photon enters a photoconductor, its energy creates an electron–hole pair in picoseconds, elevating an electron to the valence band and leaving a hole in the conduction band. Reviews of switch development are available.[9,10] Several modes of operation exist:

- In the *linear mode*, one electron–hole pair is produced for each photon absorbed, and therefore, the conductivity is linearly proportional to the total photon flux on the semiconductor material. The typical material is silicon (Si) or doped gallium arsenide (GaAs) or indium phosphide (InP). The carrier lifetime is shorter than that of the optical pulse, so switch conductivity and the output electrical pulse follow the amplitude of the optical pulse. Switching in the linear mode requires ~1 mJ/cm² of optical energy, and so means larger lasers than the other modes.
- In the *lock-on mode*, the laser causes the switch to close, but the switch opens only partway when the laser pulse ceases. The switch (GaAs, InP) recovers when the current through the circuit is shut off by a line reflection or some other circuit mechanism. In the linear mode, carriers live for only a few nanoseconds. In the lock-on mode, the carriers remain for as long as the current flows. The lock-on mode demands less laser power than the linear mode (~1 kW).
- In the *avalanche mode*, the voltage across the switch is higher, so that at a critical electric field, the switch stays closed, even with the laser off. Carrier multiplication occurs at the higher electric field, and the carriers are sustained by the switching processes. The threshold electric field in GaAs is ~8 kV/cm. The energy required to trigger the switch is reduced about two to three orders of magnitude compared to linear switching. Avalanched GaAs has become the PCSS of choice.

The *switching gain* is the ratio of the output power of a photoconducting switch to the laser power necessary to switch it. The gain achievable depends upon the switching medium; gain is greatest in the avalanche mode. For example, Nunnally[10] calculates linear mode gains in GaAs of <2, and avalanche mode gains of 10 to 100; higher values are possible. The lock-on mode has made possible the fast, subnanosecond high-current switching necessary for generation of high power UWB microwave sources. Gallium arsenide is now the most commonly used material, and the principal development issues are lifetime and power handling. The lock-on mode has substantial field in the material, which leads to filamentation of the current and burnout. The lifetime of the switch varies inversely with the power level it passes. Lifetimes are now in excess of 10^9 pulses/switch and decrease with repetition rate, pulse length, and power level. The current developments in photoconductive switching are to improve these performance measures along with switch quality. Although GaAs has become the PCSS of choice, SiC is under study as a possibility.

The most powerful PCSS UWB system was the GEM II, built by Power Spectra, Inc., using GaAs bulk avalanche semiconductor switches (BASSs).[11] The BASS module is very compact, so with a horn output, it can be arrayed to form a planer radiator as in Figure 6.9, a 12 × 12 array of BASS modules that achieved 22.4 kV/m at a 74-m range — a far voltage of almost 1.66 MV — at a repetition rate of 3 kHz. The array measured 1.6 × 1.6 × 0.86 m and weighed 680 kg. It was able to combine the multiple beams and steer the output beam ±30° by switching modules in the correct sequence.

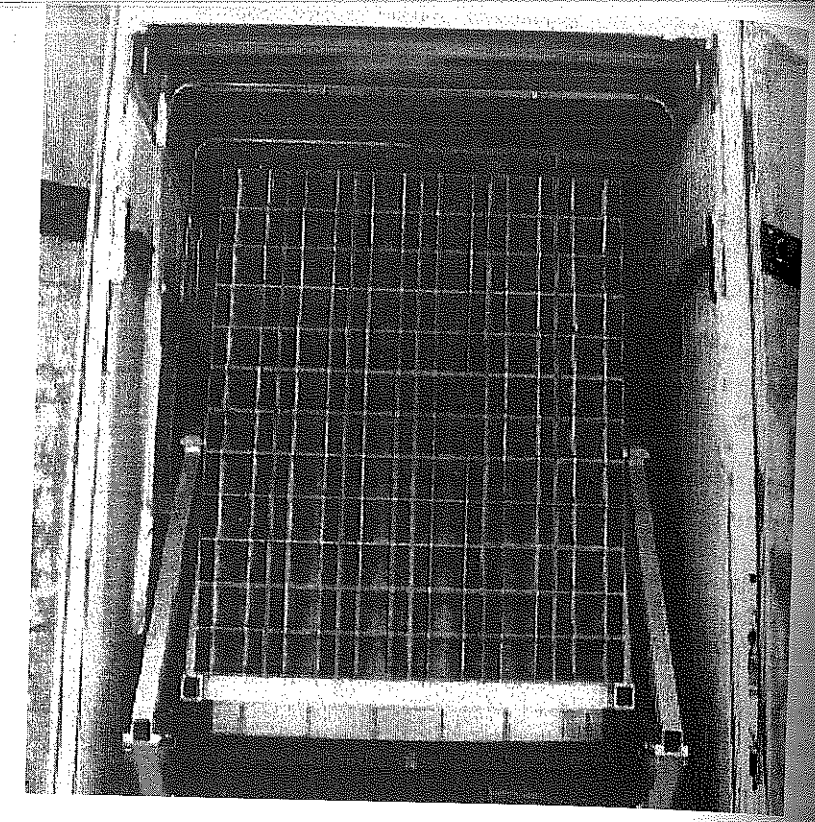

FIGURE 6.9
GEM II, an array of horn outputs driven by bulk avalanche solid-state switches mounted inside a truck. The beam formed by the array can be steered by changing the timing of the individual switches. The output pulse is similar to that in Figure 6.7.

6.3 Ultrawideband Antenna Technologies

Radiating UWB transients requires antennas specifically designed and optimized for this very demanding application. The key consideration for transient antennas is minimizing both frequency and spatial dispersion. Ordinary antennas will generally not transmit fast transients because they have not been corrected for dispersion, which follows from the fact that antenna gain varies as the square of the frequency, while UWB contains a broad range of frequencies. There were two approaches to solving this problem: modification of conventional antennas, usually TEM horns, and invention of a new type, the Impulse Radiating Antenna.

Frequency dispersion can be reduced by modification of some types of conventional antennas. This works for conical TEM horn or a biconic

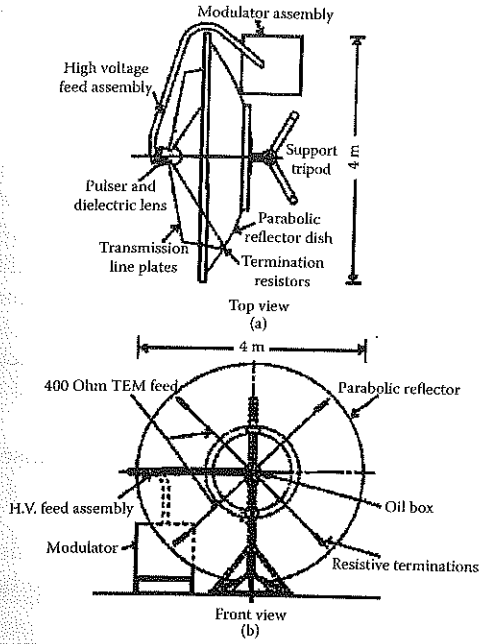

FIGURE 6.10
(a) Configuration of an IRA hyperband system, a pulser driving transmission line feeding a reflector dish. This is the prototype IRA. (b) The later IRA II. (Reprinted from Giri, D.V. et al., *IEEE Trans. Plasma Sci.*, 25, 318, 1997, Figure 1. By permission of IEEE.)

antenna, because they are frequency-independent structures that produce spherical wavefronts. However, because of the finite size of the high-voltage switches that drive them, it is often necessary to add some corrective lenses to the structure to make the wavefront more spherical.

The antenna of choice in the UWB community is the Impulse Radiating Antenna (IRA).[12] The book by Giri[1] is the most complete account, and a useful series of notes appears at Reference 13. The IRA is a means of launching a pulsed hyperband waveform onto a parabolic reflector. A pulser produces the pulse, with the final fast switch located at the focal point, which is also the apex of two transmission lines leading to the dish (Figure 6.10). The driving voltage source is ideally a step function, which in practice is a fast rise impulse with a slower decay. The TEM wave launched from the switch is guided along the conical transmission lines toward the dish. The lines are terminated at the dish, making a load for the pulser electrical circuit that is close to a match.

The key requirement of the geometry is that the dish is illuminated by a spherical TEM wave. If so, the phase center of the wave is fixed, and the IRA is dispersionless, unlike most other antennas. A nearly spherical wave reflects from the dish and propagates as a near-parallel wave into the far field. Since it comes from the focus, a spherical wave illuminating a parab-

oloidal dish reflects as a plane wave focused at infinity. The IRA concept is complex, and the detailed operation is very complex.[14,15]

The radiated field for a paraboloidal dish is

$$E(R,t) = \frac{dV_p}{dt}\frac{D}{4\pi c f_g R} \tag{6.7}$$

where dV_p/dt is the rate of change of the voltage launched by the pulser (showing the importance of rise time), D is the dish diameter, and f_g is the ratio of the impedance of the transmission lines to that of free space (377Ω). As an example, the prototype IRA system (Giri[1]) has D = 3.66 m, $dV_p/dt \sim 1.2 \times 10^{15}$ volts/sec, and $f_g = 1.06$. Therefore, at a range of 100 m the field is 110 kV/m.

The pulse in the far field has a prepulse, the main pulse, and a following undershoot. The prepulse is negative, with a duration of 2F/c, where F is the focal length of the dish.

The figure of merit adopted for UWB is the far voltage, defined in Equation 6.3. For the prototype IRA, this is 1.1 MV. The best hyperband systems have far-voltage ER products measured in megavolts.

UWB pulses propagate with considerable dispersion off axis, with the fastest pulses on axis, but slower pulse shapes at higher angles. Both rise times and durations of pulses vary with angle. The gain of impulse antennas is an issue in the community because gain in narrowband antennas is defined for single-frequency waveforms. This makes simple forms for gain and beam width difficult to define. A useful quantity somewhat like gain is the figure-of-merit far voltage (Equation 6.3 divided by the voltage on the pulser that produced it):

$$\text{UWB gain} = V_f/V_p = E(R)\,R/V_p \tag{6.8}$$

where E(R) is the time-domain peak field. For prototype IRA, $V_p \sim 115$ kV and the gain is 10.

The frequency bandwidth of the radiated field is determined by the rise time of the pulse driving the IRA and the dish diameter. The relation for the upper frequency f_u is

$$f_u\, t_r = \ln 9/2\pi = 0.35 \tag{6.9}$$

where f_u is the frequency at the upper half-power point in the spectrum and t_r is the 10 to 90 rise time of the pulse injected into the IRA. (This follows from requiring that $\omega\, t_r = 1$ and that t_r be the 10 to 90 rise time.) The lower limit of frequencies radiated has a half wavelength of about the dish diameter.

$$f_l = c/2D \tag{6.10}$$

For example, the prototype IRA has a 3.66-m dish fed by a pulse with a rise time of 129 psec, so its upper and lower frequencies are 2.7 GHz and 27 MHz, respectively.

When measuring the radiated field, how far away does one need to be to be in the far field? For UWB, the distance corresponding to the $2D^2/\lambda$ distance for narrowband (which comes from requiring that ΔR, the differential travel distance to the observer from the antenna center and edge, be λ/16) is determined by the condition that the differential travel distance be less than the rise time,

$$R/c < t_r \tag{6.11}$$

which means

$$R > D^2/2ct_r \tag{6.12}$$

For prototype IRA, R > 170 m (see Problems 4 and 5).

Building a fast hyperband IRA has complexities:

- At high voltages (>100 kV), the high-field region around the switch is usually insulated by oil and shaped to provide a lens to keep the converging wave spherical. The lens is used at the apex of the antenna to correct the astigmatism introduced by the finite size of the gas switch. With careful design, the wave is corrected by the lens to a near-spherical wavefront, so that, upon reflecting from the parabolic surface, it emerges as a plane wave.
- High-voltage hyperband pulsers producing ~0.1-nsec pulses at $\sim 10^{15}$ V/sec are difficult to design and build, but the electrical circuits are easy to model with equivalent circuit codes if the components are accurately characterized.
- IRA antennas, on the other hand, are relatively easy to fabricate, but are hard to analyze accurately.

In addition to reflector IRAs, *lens IRAs* consist of a TEM horn with a dielectric lens in the aperture. Focusing lenses at the output of TEM horns correct the nonplanarity of the wavefront and, in creating a plane wave, reduce the spatial dispersion, which increases the rise time. The lens adds substantially to the weight, so lens IRAs are used in applications with small apertures.

6.4 Ultrawideband Systems

We give notable examples of representative UWB devices, by frequency band classes.